KEYNOTE ADDRESS

PROBING ULTRAFAST BIOLOGICAL PROCESSES BY PICOSECOND SPECTROSCOPY

P. M. RENTZEPIS, *Bell Laboratories, Murray Hill, New Jersey 07974 U. S. A.*

ABSTRACT A brief discussion of the initial events leading to the visual transduction process will be presented to illustrate the capabilities of picosecond spectroscopy.

INTRODUCTION

In view of the fact that picosecond spectroscopy is a new field, at least relative to nuclear magnetic resonance (NMR) and mixing, a brief discussion of the experimental techniques seems necessary despite the wide exposure it has received since its genesis 12 years ago.

The goal of this optical system is to produce a high-quality picosecond pulse, well defined in bandwidth, energy, and time duration. This pulse will be utilized to generate the continuum that will probe the changes in absorption taking place after excitation in picosecond time intervals. The changes will then be detected, analyzed, and displayed by the diagnostics system. This apparatus is used to probe the events leading to visual perception after the absorption of a photon by the chromophore rhodopsin.

THE OPTICAL SYSTEM

Fig. 1 displays these components and the mode of utilization of each component. One of the important aspects of the system is in the generation of high-quality picosecond pulses, as developed by Huppert and myself (1). The major advantages are in the narrow bandwidth, $<3\ cm^{-1}$, coupled to a short duration, 4–6 ps, and the ease in construction. The oscillator cavity consists of a $7\frac{1}{2} \times \frac{1}{2}$ inch Nd^{3+} silicate glass rod, mode-locked by a 62% T, Kodak 9860 dye (Eastman Kodak Co., Rochester, N.Y.) in a 1-cm optical path length cell placed at the Brewster angle close to the rear mirror. The output of this laser consists of ~100 pulses per train, detected by an ITT F-4000S-1 photodiode (ITT, Electro-Optical Products Div., Roanoke, Va.) and displayed by a 519 Tektronix oscilloscope (Tektronix, Inc., Beaverton, Ore.).

From this train, a single pulse was extracted by means of a Pockels cell. The extracted single pulse was then amplified by the Nd^{3+}-yttrium aluminum garnet (YAG)

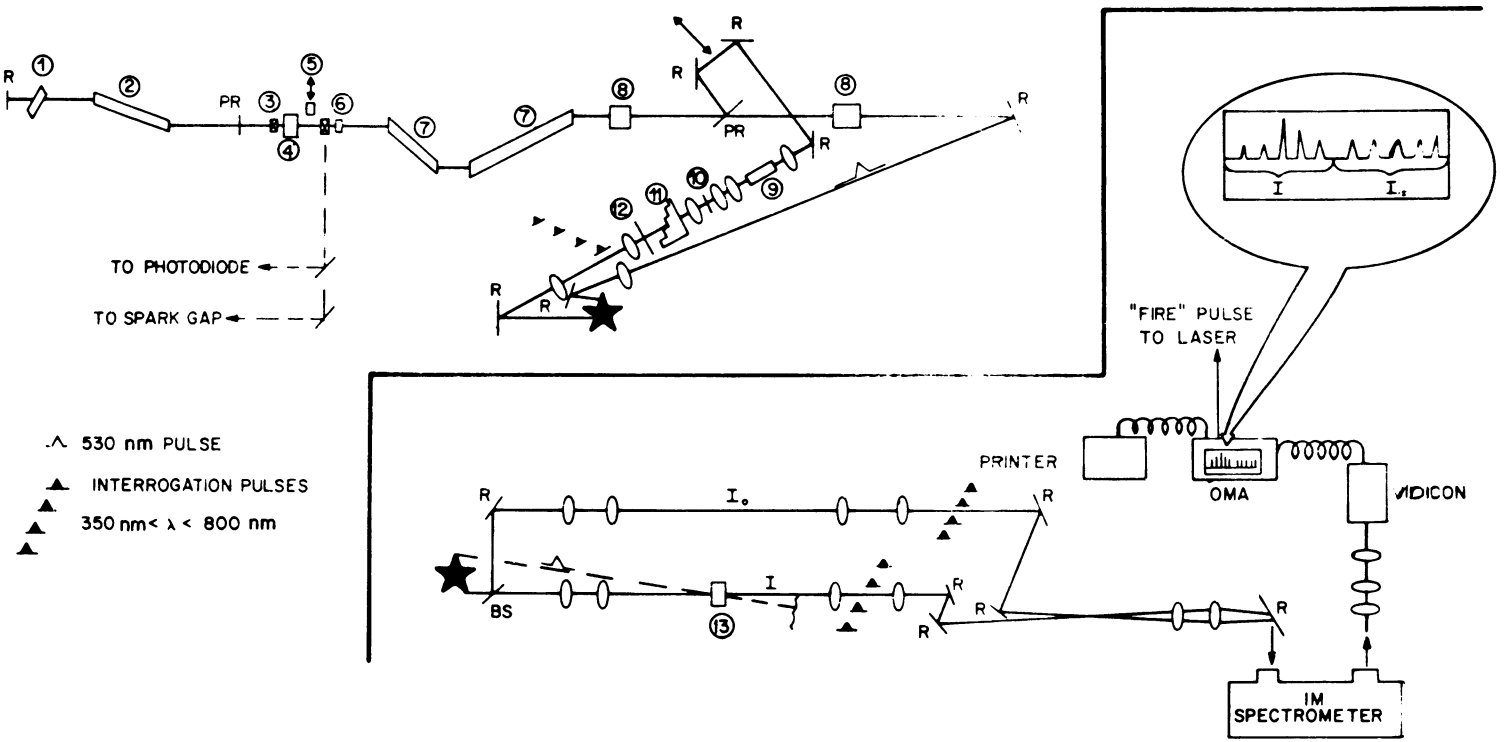

FIGURE 1 Double-beam picosecond spectrometer utilizing a silicon vidicon detector. Components: 1, mode-locking dye cell; 2, laser oscillator; 3, calcite polarizer; 4, Pockels cell; 5, translatable 90° polarization rotator for 1,060-nm radiation; 6, fixed-position 90° polarization rotator; 7, YAG amplifier rod; 8, second harmonic (530-nm) generating crystal (KDP); 9, 20 cm octanol cell for generating the interrogation wavelengths; 10, ground glass diffuser; 11, index matched glass echelon for producing picosecond optical delays between the stacked interrogation pulses; 12, vertical polarizer; 13, sample cell; R, reflector, PR, partial reflector, BS, beam splitter; OMA, optical multichannel analyzer.

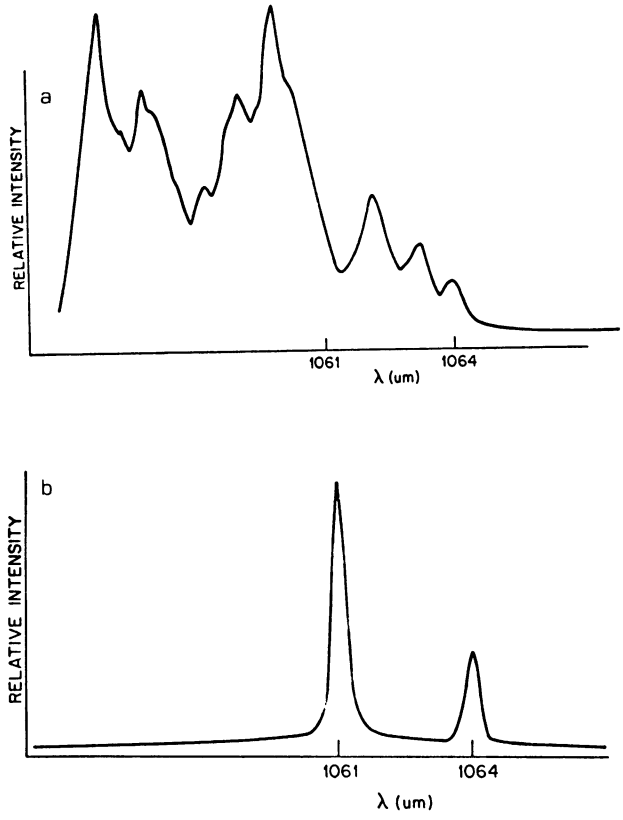

FIGURE 2 (*a*) Spectra of single-picosecond pulse emitted by the Nd^{3+}-silicate glass oscillator. The spectral structure varies within the pulses of a single train and from one shot to another. The average spectral width of Nd^{3+}-ED-2 silicate glass oscillator pulse is $\sim 100\ cm^{-1}$. (*b*) Spectra of a Nd^{3+}-glass picosecond pulse amplified by Nd^{3+}-YAG. The right-hand peak corresponds to the well-known Nd^{3+}-YAG laser line at 1,064 nm. The center peak is $\sim 30\ cm^{-1}$ shifted from the 1,064 nm, i.e., ~1,061 nm. The spectral width at half-maximum of each of these two lines is $\sim 3\ cm^{-1}$.

amplifier element (Fig. 1) consisting of a $6\frac{1}{8} \times \frac{3}{8}$-inch rod pumped by a 4-inch flash lamp. Additional amplification was provided by a $12 \times \frac{3}{4}$-inch Nd^{3+}/glass rod (Fig. 1).

The advantage of this system, devised by Huppert and myself (1), is the generation of a $3\ cm^{-1}$, 6 ps pulse. The spectrum of this pulse is shown in Fig. 2. Notice that the spectral width of the Nd^{3+} glass is larger than $100\ cm^{-1}$ (Fig. 2*a*) and exhibits a nonsymmetric structure. Each "peak" of the spectrum varies in its relative intensity, band width, and position, from one laser "shot" to another, and even from one pulse to another within a single pulse train.

The addition of the Nd^{3+} YAG rod as the amplifier, results in a frequency-selective amplification (Fig. 2*b*), which corresponds to the emission spectrum of Nd^{3+}/YAG, $\sim 3\ cm^{-1}$ and the pulse width of the Nd^{3+}/glass of 6 ps and ~800 mJ in energy. It is obvious that amplification takes place at two wavelengths, 1,064 and

1,061 nm. The full width at half-maximum (FWHM) of each of these bands is $<3\ cm^{-1}$, corresponding to a broadening of 1–2 cm^{-1} above the inherent Nd^{3+}/YAG pulse. In contrast, the Nd^{3+}/YAG-amplified pulse of the Nd^{3+}-glass laser has experienced a band width narrowing by at least a factor of 30, compared to the original Nd^{3+}-glass pulse, while retaining the short time width.

The 6 ps, $<3\ cm^{-1}$ pulse passes through a KD*P crystal generating an approximately 10 mJ, 530-nm pulse or a 640-nm stimulated Stokes-Raman pulse in 1 cm liquid. These pulses are used for excitation of the sample while a broad-band continuum born in a 10-cm cell of H_2O or alcohol(s) as a result of self-phase modulation of the laser pulse is used for interrogating the spectroscopic changes in the sample as a function of time, after passing through the echelon. The paths of these pulses in the experiment are shown in Fig. 1.

The echelon transforms the continuum into seven pulses with an interpulse separation of either 20 or 7 ps. This echelon-induced train is then split into two sets of seven segments each by a pellicle beam splitter (Fig. 1); these sets form the reference I_0 and interrogating (I) beams of the double-beam picosecond spectrometer (2). In a particular experiment, a segment of the I beam entered the sample simultaneously with the excitation, whereas the rest of the I segments entered subsequently, while the I_0 train traversed through the air or a cell containing the solvent only.

For all experiments, the echelon segments were sharply imaged onto distinct spatial regions of a N_2-cooled silicon vidicon. The horizontal vidicon axis (x axis) provided

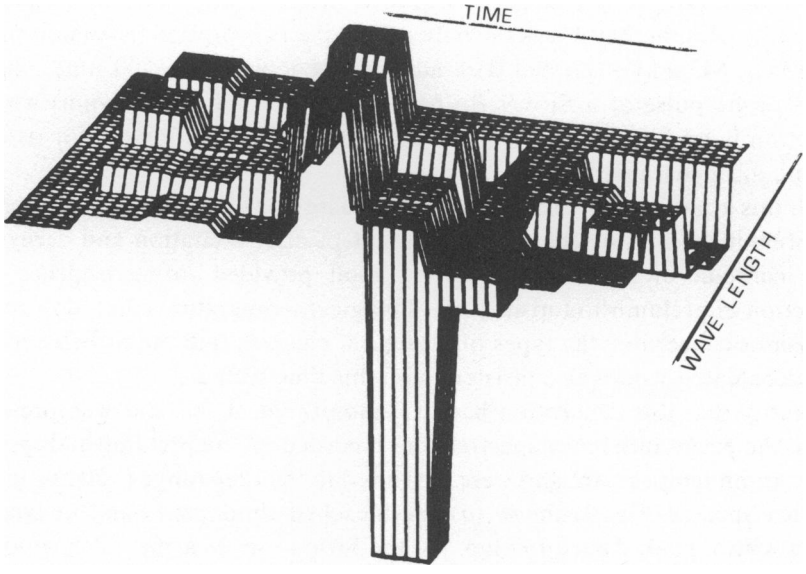

FIGURE 3 Three-dimensional display (τ, λ, ΔOD) of the optical density changes after excitation with a picosecond pulse at 530 nm. The wavelength range displayed is between 570 and 550 nm, the time in 10-ps segments covers 100 ps, and the optical density ranges from −0.6 to 0.3 OD.

the wavelength coordinate, while the vertical axis (along the spectrometer entrance slit, y axis) formed the time element.

The data are displayed either in a plot of τ (in picoseconds) vs. I, or three-dimensionally as shown in Fig. 3, in the form of time in picoseconds (x axis) versus wavelength in nanometers (y axis) versus intensity (z axis). ΔA was calculated for each time (echelon) segment by evaluating $\Delta A + \log (I^w/I^n)$, in which I^w and I^n refer to the intensity of the interrogating pulse in the presence and in the absence of the excitation pulse, respectively. The effect of excitation intensity and reliability of the data becomes more evident by considering that in most experiments discussed, the ratio of ΔA with and without excitation is ~ 10 – i.e., $\Delta A_{(\text{with})} = 0.3$ and $\Delta A_{(\text{without})} = 0.03$. This system, with obvious variations, was utilized in the study of many ultrafast processes, including the primary processes in vision.

PRIMARY PROCESSES IN RHODOPSIN

Prior stationary studies at low temperature have shown that the intermediate, prelumirhodopsin (prelumi), is formed first, decaying into lumirhodopsin, followed by the intermediates meta I and meta II (3–5). The first intermediate, prelumirhodopsin, was identified at low temperatures; however, its physiological temperature kinetics were unknown because of its rapid formation and decay. Later-forming transients were found to be *trans* isomers of the original *cis*-rhodopsin, and therefore a number of workers (6) assumed that the initial action of light caused isomerization of the retinal and thus the prelumirhodopsin intermediate was a *trans* isomer of rhodopsin.

The earliest species observed in the sequence, prelumirhodopsin, was unique among the intermediates, in that it was the only one with an absorption maximum shifted to the red (λ_{max} 543 nm) of normal dark-adapted rhodopsin (λ_{max} 500 nm). Thus, by using a probe pulse at a Stokes-Raman shifted wavelength (561 nm) within the absorption band for prelumirhodopsin, it was possible to monitor for its appearance and disappearance.

With this approach, an absorbing intermediate was observed (7) and interpreted to be prelumirhodopsin. It appeared within 6 ps after excitation and decayed with a time constant of about 50 ns. This result provided strong evidence for the production of prelumirhodopsin at physiological temperatures and also permitted conclusions concerning the types of structural changes that might be occurring in the molecule that would be consistent with this time scale.

To verify that this absorption band (7) monitored at 560 nm was prelumirhodopsin, the entire difference spectra were recorded of the prelumirhodopsin spectrum at room temperature and were measured in the time range 6–300 ps (8). This difference spectra (Fig. 4) shows (*a*) the bleached rhodopsin band between 430–510 nm with a peak ΔA at 485 nm, (*b*) the formation of a new absorption band at 530–680 nm with a maximum at 580 nm, (*c*) an isobestic point at 525 nm, (*d*) the rhodopsin bleached within 6 ps and the prelumirhodopsin band also formed within 6 ps. To elucidate the mechanism and resolve the rate of formation of prelumirhodopsin, we repeated these studies at lower temperatures. Such experi-

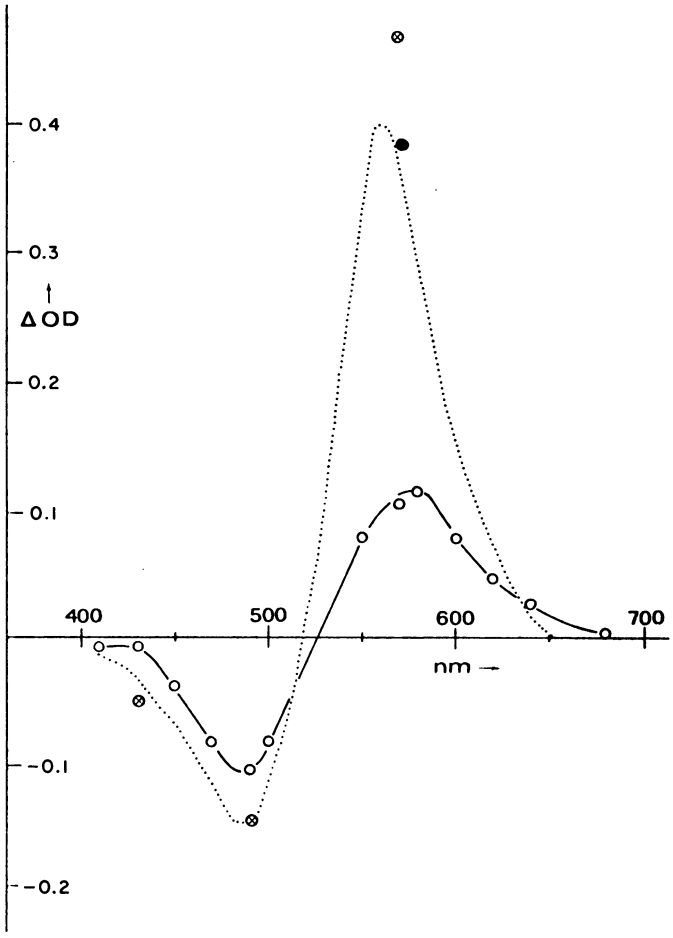

FIGURE 4 Prelimirhodopsin difference spectrum. ○, recorded at 298°K, 60 ps after excitation with a 5-mJ pulse at 530 nm (4); ●, 77°K, and ⊗ 4°K (this work); . . . ; difference spectrum generated by photostationary studies of low-temperature glasses for 77° and 7°K. Photostationary studies at 77° and 7°K give identical difference spectra. The data is normalized to concentrations used for this kinetic study. Rhodopsin was solubilized in 0.3 M Ammonyx (cetalkonium chloride, Onyx Chemical Co., Jersey City, N.J.)-0.01 M Hepes at pH 7.0; $A_{500} = 0.73$ in a 2 mm path.

ments between 300° and 4°K reveal that at as low as 77°K the rise time of the band at 570 nm is still less than 10 ps and only below 30°K could a resolvable lifetime be observed (9). Even at 4°K the rise time was only 36 ps as shown in Fig. 5.

To elucidate these data, which were not expected if one assumed that the isomerization mechanism were responsible for the formation of prelumirhodopsin at low temperatures, the rhodopsin was immersed in D_2O to substitute all exchangeable protons with deuterium. It is well known that the hydrogens of the retinal chromophore do not exchange, except for the proton of the protonated Schiff base, which easily exchanges

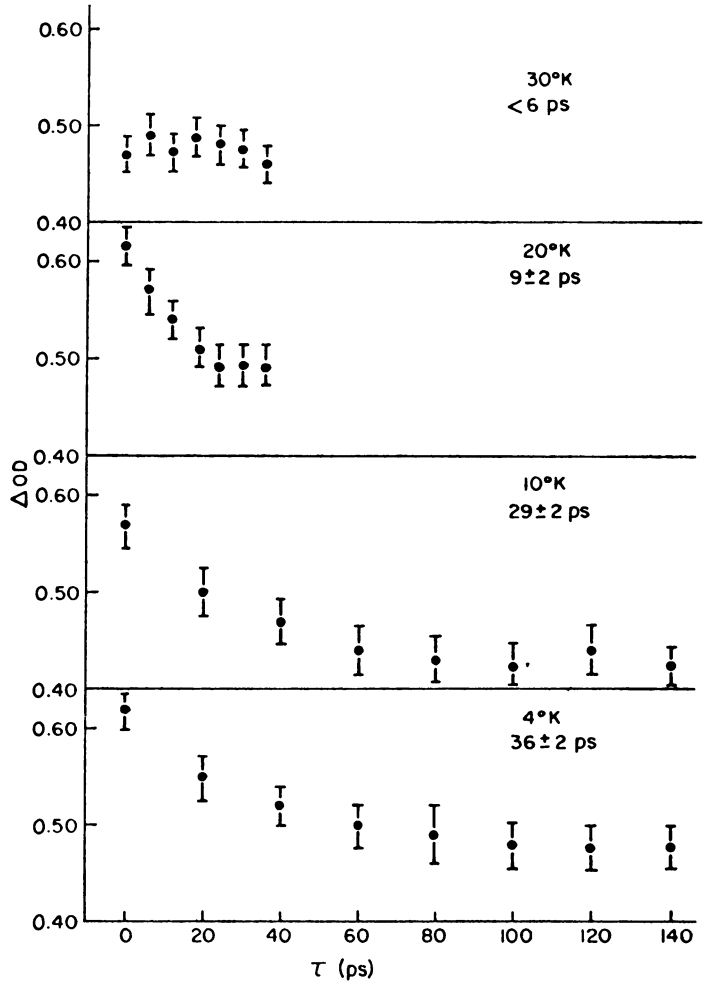

FIGURE 5 Kinetics of formation of prelumirhodopsin at various temperatures monitored at 570 nm. Excitation of rhodopsin was with a 5-mJ, 530-nm, 6-ps pulse. The glass for low-temperature study was formed by mixing one part rhodopsin, solubilized in 0.3 M Ammonyx-0.01 M Hepes at pH 7.0, $A_{500} = 10.0$, with two parts distilled ethylene glycol. The lifetime for formation, given in the upper right of each panel, is the reciprocal of the rate constant obtained by a least-square fit of $I_n (A_t - A_\infty)$ versus time, t, in picoseconds; A is absorbance at 570 nm.

for deuterium in D_2O (10). The rationale for the deuterated experiment was that if isomerization of the retinal is responsible for the observed kinetics, then deuterium substitution will not cause a major change in the rates, since at the point of isomerization, the retinal protons have not been replaced by deuterium.

However, the deuterated rhodopsin showed rates for the formation of prelumirhodopsin much slower than its protonated homologue. For example, at 570 nm D-rhodopsin exhibits a formation lifetime for prelumi of 17 ps at 4°K and, as the temperature decreases. this rate achieves values ranging from 51 ps at 30°K to 256 ps at

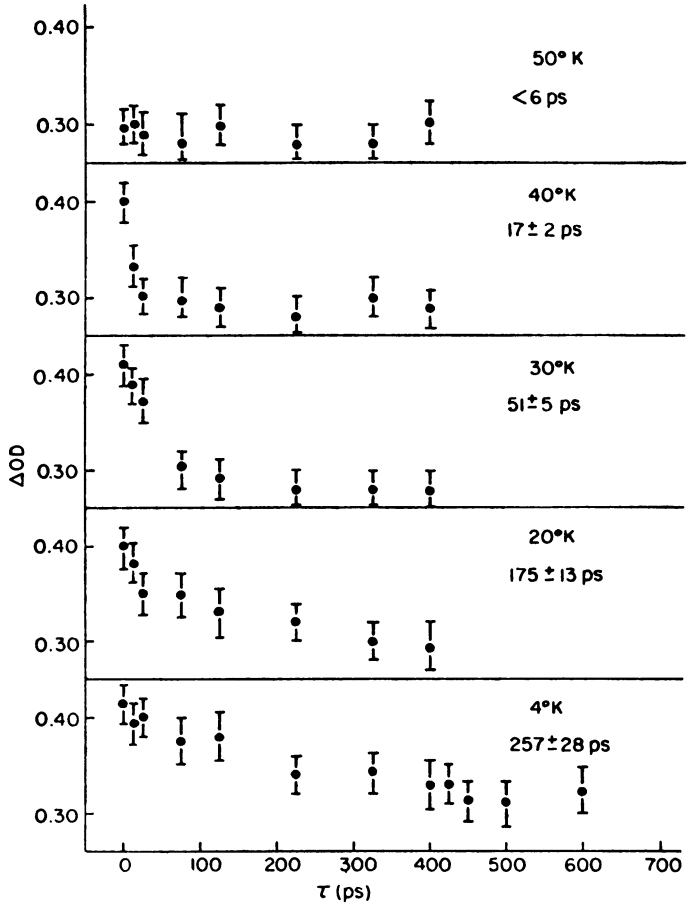

FIGURE 6 The kinetics of formation of deuterium-exchanged prelumirhodopsin at various wavelengths. The excitation of deuterium-exchanged rhodopsin was with a 5-mJ, 530-nm, 6-ps pulse. The glass for low temperature study was formed by mixing one part D-rhodopsin in deuterium-exchanged 0.1 M Ammonyx/0.01 M Hepes at pH 7.0, $A_{500} = 7.0$, with two parts deuterium-exchanged ethylene glycol. The lifetime of formation was calculated as for Fig. 5.

4°K (Fig. 6). This behavior is in clear contrast to the H-rhodopsin, prelumi formation with lifetimes of 9 ps at 30°K to 36 ps at 4°K (Fig. 5).

A transient species also appeared that decays fast into a long-lived species absorbing at 570 nm. We believe that this is an excited singlet state of rhodopsin prepared by the 530-nm excitation pulse.

PROTON TRANSLOCATION

The conversion of rhodopsin into prelumi via the excited state is a very efficient process, since no significant rhodopsin ground state repopulation is observed during the first 100 ps after excitation. Information concerning the mechanism responsible for the

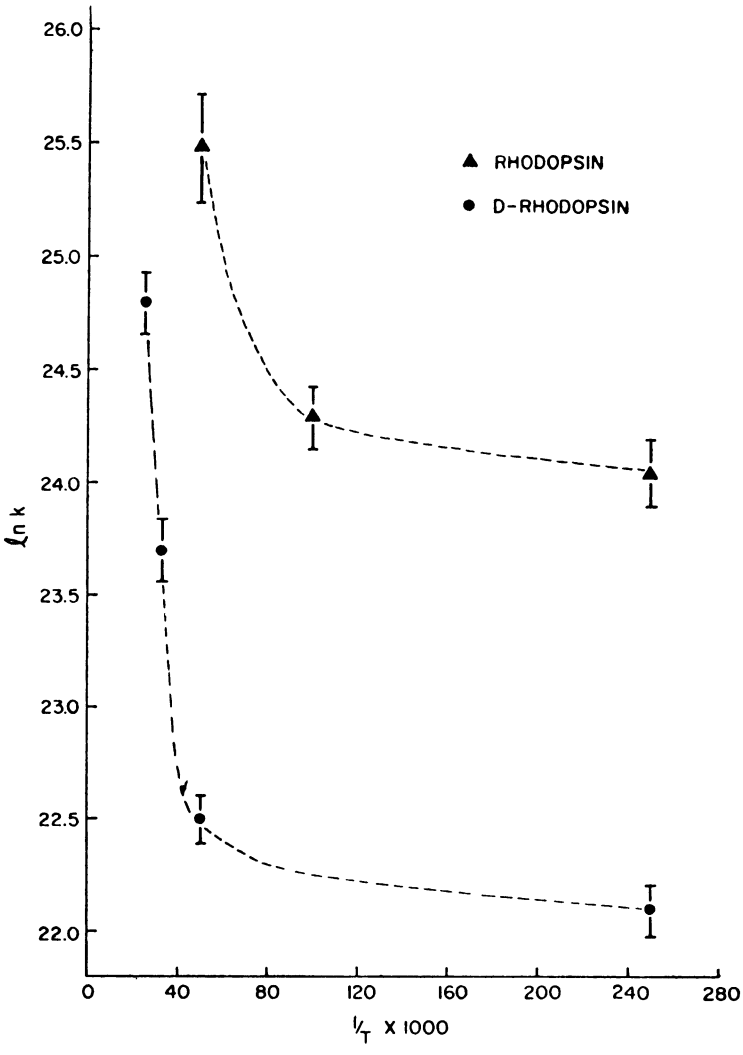

FIGURE 7 An Arrhenius plot, ln k for formation of prelumirhodopsin versus $1/T$ (L) × 10^3, of the kinetic data in Figs. 5 and 6. The value of ln k = 25.84 corresponds to a lifetime of 6 ps.

formation of prelumi can be obtained by a closer examination of the temperature dependence of the formation rate constant K_{PL} of prelumi and its isotope dependence. Fig. 7 shows the temperature dependence of K_{PL} plotted in the Arrhenius form (ln k vs. $1/T$). Two striking features of this plot are immediately apparent: (*a*) the curve results from ln K_{PL} vs $1/T$ is not a straight line, as expected for an Arrhenius process. (*b*) At the limit of $T = 0$, K_{PL} is finite and temperature independent.

The effect of deuteration on K_{PL} is to make the rate slower in D- vs. H-rhodopsin with a ratio $K_{PL}^{H}/K_{PL}^{D} \approx 7$. Since only the proton of the protonated Schiff base

is exchangeable in the retinal sequence, in the absence of drastic changes of the protein structure by D_2O, the observed isotope dependence suggests a tunneling process (11). Proton tunneling has indeed been proposed to take place in some excited state proton transfer reactions. The data on temperature and isotope dependence strongly suggest a proton transfer reaction as being mainly responsible for the formation of prelumi at low temperatures. That the absorption spectrum of prelumi is red-shifted with respect to the spectrum of rhodopsin itself suggests that prelumi may be a more tightly protonated Schiff base than rhodopsin. Model studies (12) indicate that translocating the proton towards the Schiff base nitrogen could account for the spectral red shift.

The mechanism of formation of prelumi at higher temperatures has been described as a *cis-trans* isomerization. The extremely fast formation of prelumi at 4°K, though, argues against such an isomerization process, at least at low temperatures. Several studies have shown (13) that as the temperature is decreased, the quantum yield of photoisomerization of retinal analogues and retinal Schiff bases decreases, and at 77°K photoisomerization ceases completely, as does the isomerization of stilbene (14). However, we must make it clear that the mechanism of the formation of prelumi at higher temperatures cannot be ascertained by the available results. Regarding the mechanism for the proton translocation process, the existing theories are not sufficiently refined to give an exact answer. However, assuming that the expression provided (11),

$$k_t = \nu_0 \exp \frac{-\pi^2 a_0 k_t}{b} (2ME_a)^{1/2}, \tag{1}$$

is applicable to rhodopsin, we can calculate an activation energy or barrier height, E_a, and a width of the barrier or translocation distance a_0. Using the experimental rate constant of 2.8×10^{11} s^{-1} at 4°K, and the normal value ν_0, and the mass of the proton M, we calculate an E_a value of 1.4 kcal if we give ν_0 the N—H band frequency of 1,500 cm^{-1}. If we use instead the more reasonable value of 10^{13} for the frequency of the translocated proton, then we have a barrier of 740 kcal or a height ~100 cal above room temperature. This indicates that at room temperature the proton translocation could be an activated process proceeding without a barrier. This would explain the ultrafast rate observed for the formation of prelumi at room temperature. Similarly the distance, a_0, through which the proton tunnels is calculated to be ~0.5 Å.

MODELS FOR PROTON TUNNELING

The kinetic data reported originally by Peters et al. (9) are consistent with at least two proton translocation mechanisms: (*a*) A concerted double hydrogen transfer leading to a retro-retinal structure, a slightly different mechanism than the one proposed previously (15). (*b*) A single proton translocation to the Schiff base nitrogen generating a carbonium ion, as proposed by Mathies and Stryer (16). The proton translocation is thought to be facilitated by an active role of an amino acid, with histidine being a

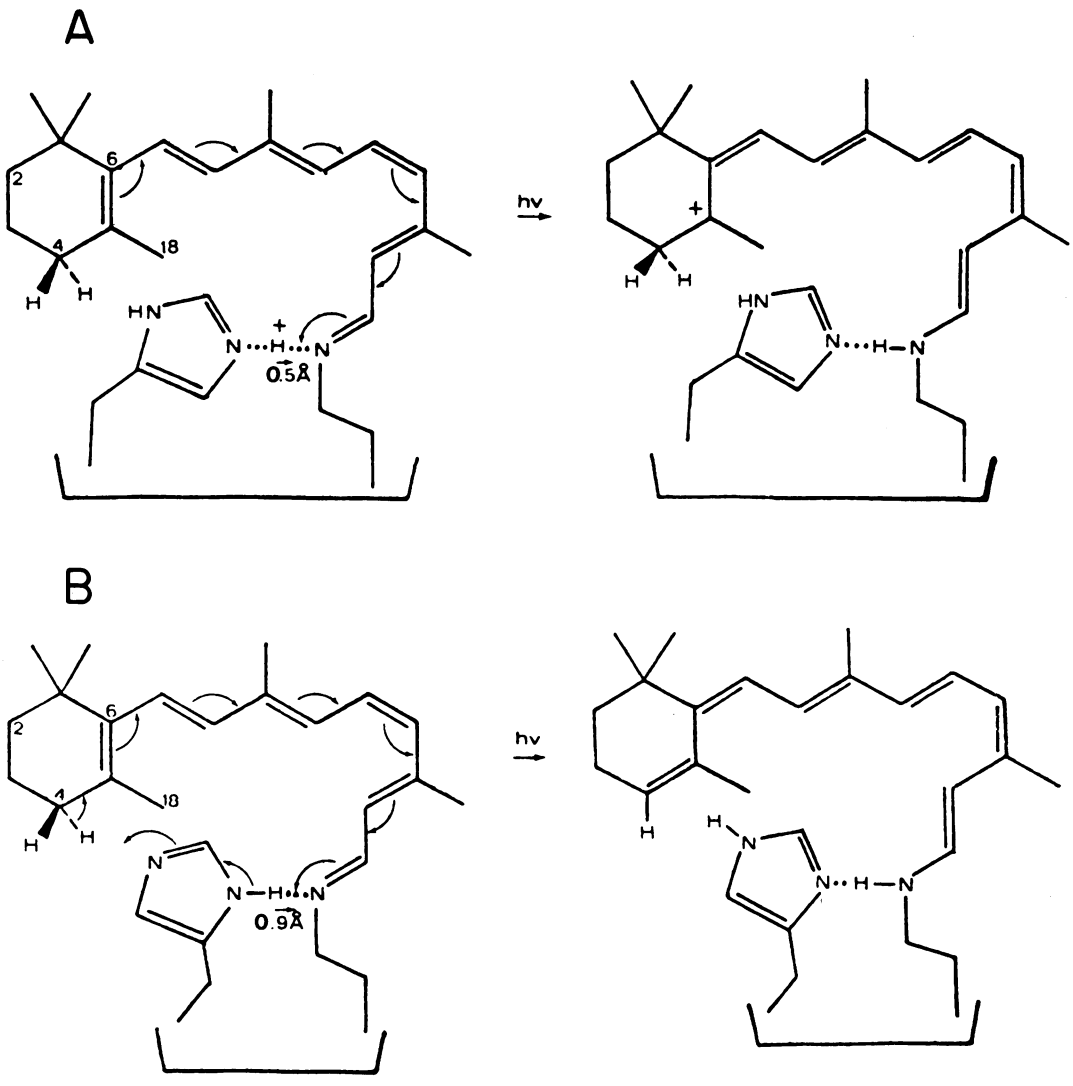

FIGURE 8 Models for proton translocation to form prelumirhodopsin: A, single proton translocation with carbonium ion formation; B, concerted double proton translocation with retroretinal formation. The tunneling distances, a_0, through the barriers for the formation of prelumirhodopsin are 0.5 Å for single proton model A and 0.9 Å for the concerted double proton translocation.

strong candidate (Fig. 8). At the present time, we can postulate several other candidates and mechanisms involving the proton; however, until more definitive data is available, we shall limit our proposals to the above two models, presented schematically in Fig. 8. If the histidine proton is translocated, this would occur between the hydrogen-bonded nitrogens of the histidine and Schiff base, and the proton would translocate along the N—H stretch coordinate, moving near the Schiff base nitrogen,

which has been said to have a "negative" character in the excited state and provide the force for the proton movement. If the proton is originally shared by the two nitrogens $N_h \cdots H \cdots N_S$, the translocation distance will be ~0.5 Å, while if the proton is held strongly by the histidine nitrogen $N_h—H \cdots N_S$, then the distance for translocation would be ~0.9 Å. Under these conditions there would be no need for an immediate hydrogen abstraction for carbonium ion stabilization. In the two-photon model, stabilization can be achieved by the removal of a hydrogen from an adjacent carbon. Protein conformational changes would be affected by the proton translocation; however, their magnitude and rate, especially at very low temperatures, would not be expected to be very high. I can only conclude from the available data that proton tunneling plays a dominant role in the formation of prelumirhodopsin, at least at low temperatures. The exchanges of D for H strongly support, if not confirm, our tunneling proposal and shows that proton tunneling indeed takes place. Which proton? The present data do not provide an unequivocal answer.

REFERENCES

1. HUPPERT, D., and P. M. RENTZEPIS. 1978. *Appl. Phys. Lett.* **32**:241.
2. NETZEL, T. L., and P. M. RENTZEPIS. 1974. *Chem. Phys. Lett.* **29**:337.
3. YOSHIZAWA, T., and Y. KITO. 1958. *Nature (Lond.).* **182**:1604.
4. YOSHIZAWA, T., and G. WALD. 1963. *Nature (Lond.).* **197**:1279.
5. YOSHIZAWA, T. 1972. *In* Handbook of Sensory Physiology. H. Dortnell, editor. Springer-Verlag KG. Berlin. Vol. VII/I, 146–179.
6. ROSENFELD, T., B. HONIG, M. OTTOLENGHI, and T. G. EBREY. 1977. *Pure Appl. Chem.* **49**:341.
7. BUSCH, G. E., M. L. APPLEBURY, A. A. LAMOLA, and P. M. RENTZEPIS. 1972. *Proc. Natl. Acad. Sci. U.S.A.* **69**:2802.
8. SUNDSTROM, V., P. M. RENTZEPIS, K. S. PETERS, and M. L. APPLEBURY. 1977. *Nature (Lond.).* **267**:645.
9. PETERS, K., M. L. APPLEBURY, and P. M. RENTZEPIS. 1977. *Proc. Natl. Acad. Sci. U.S.A.* **74**:3119.
10. OSEROFF, A., and R. CALLENDER. 1974. *Biochemistry.* **13**:4243.
11. LOWDIN, P. O. 1965. *Adv. Quantum Chem.* **2**:213.
12. WADDELL, W., and R. S. BECKER. 1971. *J. Am. Chem. Soc.* **93**:3788.
13. WADDELL, W., A. M. SCHAEFFER, and R. S. BECKER. 1973. *J. Am. Chem. Soc.* **95**:8233.
14. SALTIEL, J., J. D'AGOSTINO, E. D. MEGARITY, L. METTS, K. R. NEARBERGER, M. WRIGHTON, and O. I. ZAFIRIOU. 1973. *Org. Photochem.* **3**:1.
15. VON DER MEER, K., J. J. C. MULDER, and J. LUGSTENBURG. 1976. *Photochem. Photobiol.* **24**:363.
16. MATHIES, R., and L. STRYER. 1976. *Proc. Natl. Acad. Sci. U.S.A.* **73**:2169.

DISCUSSION

WELLER: With your diagram of the proton tunneling from excited rhodopsin to prelumi, do you indicate that an adiabatic proton transfer process occurs from excited singlet state to singlet excited prelumi, or do you consider it to be an adiabatic process leading from singlet excited rhodopsin directly to the ground state of prelumi?

RENTZEPIS: We believe that tunneling takes place in the excited state. Prelumi decays thereafter to lumi with a 50 ns lifetime.

FARRAGI: You've measured the pH effect?